JOURNAL OF CHEMICAL INFORMATION AND MODELING

Article

pubs.acs.org/jcim

Computational Modeling of Kinesin Stepping

Hamidreza Khataee* and Alan Wee-Chung Liew*

School of Information and Communication Technology, Gold Coast Campus, Griffith University, Gold Coast, Queensland 4222, Australia

ABSTRACT: Kinesin is a walking motor protein that shuttles cellular cargoes along microtubules (MTs). This protein is considered as an information processor capable of sensing cellular inputs and transforming them into mechanical steps. Here, we propose a computational model to describe the mechanochemical kinetics underlying forward and backward stepping behavior of kinesin motor as a digital circuit designed based on an adenosine triphosphate (ATP)-driven finite state machine. Kinetic analysis suggests that the backward stepping of kinesin is mainly driven by ATP hydrolysis, whereas ATP synthesis rises the duration of this stepping. It is shown that kinesin pausing due to waiting for ATP binding at limiting ATP concentration ([ATP]) and low backward loads could be longer than that caused by low rate of ATP synthesis under high backward loads. These findings indicate that the pausing duration of kinesin in MT-bound (M·K) kinetic state is affected by [ATP], which in turn affects its velocity at fixed loads. We show that the proposed computational model accurately simulates the forward and backward stepping behavior of kinesin motor under different [ATP] and loads.

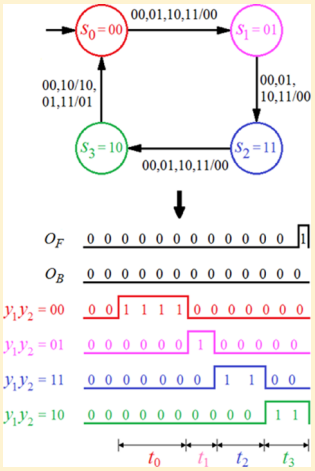

1. INTRODUCTION

Conventional kinesin is a double-headed and adenosine triphosphate (ATP)-driven motor protein that walks processively in discrete 8.2 nm steps[1] and in an asymmetric hand-over-hand fashion toward the plus end of microtubules (MTs)[2,3] in the presence of ATP or in the absence of ATP if external load is applied to the motor.[2] Kinesin stepping exerts localized forces on nanostructures, and thus can be exploited in nanorobotics[4] by designing synthetic nanodevices powered by kinesin[5−7] and in the controlled propagation architecture of nanonetworks in which information molecules are carried by kinesin motors between transmitter and receiver nanomachines.[8,9] Synthetic nanodevices and nanonetworks are anticipated to contribute in medical diagnostics as well as engineering applications.[5,6,8] Despite this progress, artificial nanomotors still lack the functionality and efficiency of their biological counterparts.[10−12] One of the issues frequently raised in designing nanodevices with capability of molecular communication and computing is the connectivity of molecules when the output from one molecule is used to control another.[13]

Kinesin is considered to be a basic protein nanomachine capable of sensing, processing information, and actuating.[9−11] Meanwhile, the mechanical kinetics driving kinesin motion are fundamentally different from those of macroscopic motors.[14] Representing the mechanical kinetics underlying the stepping cycles of kinesin using computational logic models used to model the control flow of macroscopic systems' behaviors would allow us to describe how the cellular inputs sensed by kinesin are transferred into mechanical steps. Modeling the processing unit of a molecule using computational techniques is particularly important for representing the information handling in an assembly of molecules, each with its own function, where the output from one molecule is used to control another.[13] Recently, we developed a mathematical model for describing the mechanical kinetics of kinesin stepping.[15] We showed that the model could be used to analyze, conceptualize, and predict forward and backward stepping of kinesin motor in different ATP concentrations ([ATP]) and loads. On the basis of our findings in ref 15, we then developed a stochastic automaton model for simulating kinesin processivity.[16] Consequently, following our results in ref 15, we here propose a computational model for describing the mechanical kinetics underlying individual forward and backward stepping cycles of single kinesin motor as a digital circuit implementing a finite state machine (FSM)[17] (forward and backward steps are taken toward plus and minus ends of MT, respectively). FSMs are used to demonstrate the control flow of a system's behavior, whereas digital circuits map the functional description of a FSM into a logic representation in terms of logic variables and operations.[18] The theoretical foundation of the designed digital circuit is based on a discrete stochastic model of kinesin motor at various [ATP] and loads. We show that the proposed computational model, as a processing unit model actuating kinesin steps, accurately simulates the forward and backward stepping behavior of kinesin motor under different situations.

Received: August 3, 2014
Published: November 15, 2014

dx.doi.org/10.1021/ci500673z | J. Chem. Inf. Model. 2014, 54, 3439−3445

2. MODEL DESCRIPTION

2.1. Theoretical Foundation. We use the simplest four-state discrete stochastic model of kinesin motor to define single forward and backward stepping cycles of the motor

$$0 \underset{w_1}{\overset{u_0}{\rightleftarrows}} 1 \underset{w_2}{\overset{u_1}{\rightleftarrows}} 2 \underset{w_3}{\overset{u_2}{\rightleftarrows}} 3 \underset{w_0}{\overset{u_3}{\rightleftarrows}} 0$$

where

$$0 = \mathrm{M{\cdot}K}, \quad 1 = \mathrm{M{\cdot}K{\cdot}ATP}$$

$$2 = \mathrm{M{\cdot}K{\cdot}ADP{\cdot}P_i}, \quad 3 = \mathrm{M{\cdot}K{\cdot}ADP}$$

where M·K denotes the MT-kinesin complex, and the ADP·P_i complex stands for the products of ATP hydrolysis: adenosine diphosphate (ADP) and inorganic phosphate (P_i). In this four-state stochastic model, kinetic state i may transit to states i+1 and i-1 with forward and backward transition rates u_i and w_i (i = 0, 1, 2, 3), respectively, influenced by the temperature T and external forward (negative) or backward (positive) load F as

$$u_i^F = u_i^0 e^{-\theta_i^+ Fd/k_B T} \tag{1}$$

$$w_i^F = w_i^0 e^{+\theta_i^- Fd/k_B T} \tag{2}$$

where u_i^0 and w_i^0 are the transition rates at zero load, θ_i^+ and θ_i^- are the characteristic distances for the load, d is the step size (equal to 8.2 nm), and k_B is the Boltzmann constant.[19,20] The parameter values of eqs 1 and 2 summarized in Table 1 as well

Table 1. Estimated Parameters of Forward and Backward Transition Rate Equations[19]

state i	u_i^0 (s^{-1})	w_i^0 (s^{-1})	θ_i^+	θ_i^-
0			0.120	0.430
1	580	40	0.020	0.130
2	290	1.6	0.020	0.130
3	290	40	0.020	0.130

as the parameter values of [ATP]-dependent rates presented in eqs 3 and 4 have been estimated by Fisher and Kolomeisky[19] through regression on the experimental data of Block and colleagues in refs 21 and 22 at room temperature

$$u_0^0 = k_0[\mathrm{ATP}] \tag{3}$$

$$w_0^0 = k_0'[\mathrm{ATP}]/\sqrt{1 + [\mathrm{ATP}]/c_0} \tag{4}$$

where k_0 = 1.8 μM^{-1} s^{-1}, k_0' = 0.225 μM^{-1} s^{-1}, c_0 = 16 μM, and no side load has been considered.

The theory of discrete stochastic model above asserts that forward stepping of kinesin motor hydrolyzes ATP, whereas backward stepping could resynthesize ATP.[19,20,23] Experimental observations measured the stall force (F_{stall}) ranging between 5.5 and 7.6 pN[2,22,24,25] as the load point that the stepping direction of kinesin motor changes, where (*i*) below stall, forward stepping is more frequent, (*ii*) at stall, forward and backward stepping are equally likely, and (*iii*) above stall, backward stepping is dominant.[24,25] In discussing backward stepping under high backward loads, Carter and Cross[24] stated that backward stepping is unlikely to result in ATP synthesis. However, Fisher and colleagues[23] remarked that the experimental observations in ref 24 rest on a misconception of the significance of dwell times before forward and backward stepping and that backward stepping could result in ATP synthesis. In addition, in a set of theoretical works, Wang and colleagues[26−28] developed numerical algorithms based on a continuous Markov process for analyzing transport behavior of kinesin, where the jump rates were derived from local solutions of the continuous system. These approaches are followed by a numerical exploration of kinesin's neck linker extensions and modeling of kinesin movement along MT in ref 29. A general framework was also proposed to analyze time traces of the bead displacement in single molecule bead-motor assays of motor proteins in ref 30. Although these works provide a general framework to study kinesin transport mechanism, modeling the kinetics driving single stepping cycles of the motor is still lacking. Meanwhile, based on the four-state discrete stochastic model, we recently modeled the probabilities of ATP-driven forward and backward stepping of kinesin motor and, in accordance with several sets of experimental and theoretical findings,[1,2,24,25,31−33] showed that[15] (*i*) the stall force seems to be almost constant and [ATP]-independent and (*ii*) backward stepping is related to both ATP hydrolysis and synthesis with rate limiting factor being ATP synthesis. Based on these results, we here focus on the mechanochemical kinetics underlying forward and backward stepping behavior of kinesin motor and propose a computational model for representing these kinetics using logical operations and variables.

To recognize whether ATP hydrolysis or ATP synthesis kinetic cycle is dominant at loads $F > F_{stall}$ where backward stepping is more frequent, we compute the rates of forward and backward kinetic transitions using eqs 1 and 2 (see Figure 1A).

A

	Rate (s^{-1})		
	F = 8 pN	F = 9 pN	F = 10 pN
u_0	25.71	20.16	15.80
w_0	8919.86	21325.59	50985.21
u_1	419.34	402.68	386.68
w_1	329.31	428.59	557.81
u_2	209.67	201.34	193.34
w_2	13.17	17.14	22.31
u_3	209.67	201.34	193.34
w_3	329.31	428.59	557.81

B

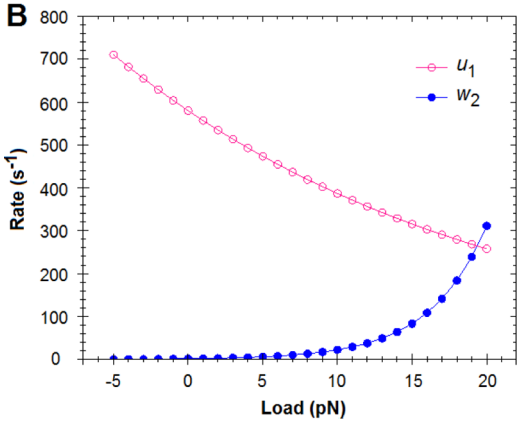

Figure 1. Kinetic transition rates for the ATP hydrolysis and synthesis cycles. Transition rates u_i^F and w_i^F at force F are depicted as u_i and w_i, respectively, where i = 0, 1, 2, 3. (A) Rates of forward and backward kinetic transitions calculated at loads $F_{stall} < F \leq 10$ pN and [ATP] = 100 μM. (B) Transition rates of ATP hydrolysis and synthesis, i.e. u_1 and w_2 respectively, versus load. ATP synthesis rate gradually increases and crossovers ATP hydrolysis rate at high backward load around 19.4 pN, above F_{detach}.

dx.doi.org/10.1021/ci500673z | J. Chem. Inf. Model. 2014, 54, 3439−3445

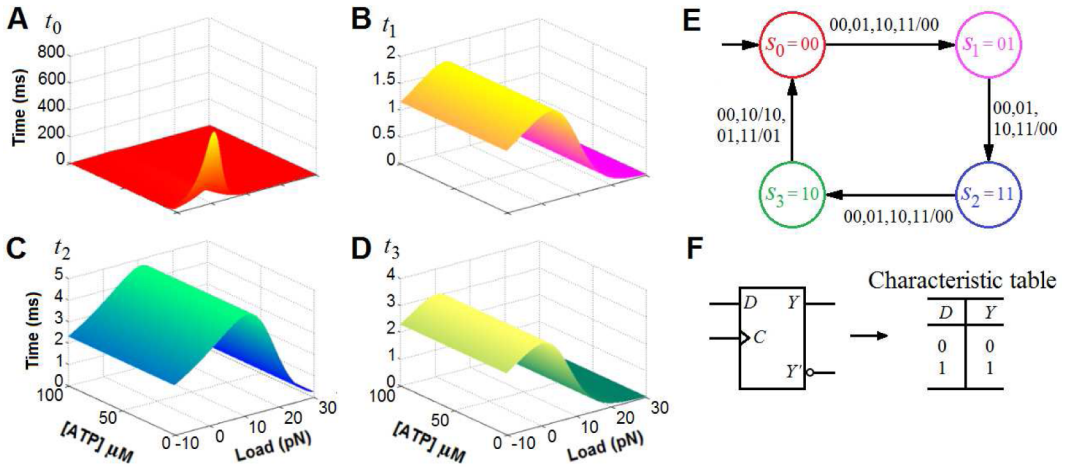

Figure 2. Durations of the kinetic states, FSM $M_{kinesin}$ and D flip-flop. (A-D) Durations of the kinetic states, t_i where i = 0, 1, 2, 3, versus [ATP] and load, respectively. (E) $M_{kinesin}$: input and output values are shown as x_1x_2/O_FO_B. States s_0 to s_3 are depicted in red, pink, blue, and green colors, respectively. The incoming unlabeled arrow to state s_0 indicates this state as the initial state. (F) D flip-flop:[45] logic diagram of the D flip-flop consists of two inputs and two outputs. Characteristic table of the D flip-flop shows that the next state of the flip-flop is obtained directly from the input D.

Our calculation shows that with increasing the load to high backward loads the rates of backward kinetic transitions w_i^F increase and crossover their respective forward kinetic transition rates u_i^F at loads $F \leq 10$ pN where i = 0, 1, 3, whereas the backward kinetic transition rate w_2^F crossovers its respective forward kinetic transition rate u_2^F at load around 17.1 pN. Due to the more frequent detachment of kinesin motor from MT at loads above 10 pN,[24] $F_{detach} > 10$ pN, our results in Figure 1A indicate ATP synthesis rate, i.e. w_2^F, as the rate limiting factor for ATP synthesizing cycle, as shown in ref 15. Figure 1A, B also indicates that at loads $F_{stall} < F < F_{detach}$, where the backward stepping of kinesin is dominant, the rate of ATP hydrolysis u_1^F is at least 17 times greater than that of ATP synthesis, w_2^F. Collectively, these results imply that the backward stepping mainly related to ATP hydrolysis as in forward stepping and is consistent with the experimental and theoretical findings in refs 24, 25, and 32. The small rate of ATP synthesis in our analysis, nevertheless, supports the theory in refs 19, 20, and 23 that backward stepping could resynthesize ATP. Forward and backward motion of kinesin has been further observed by Yildiz and colleagues[2] in the direction of the applied load and in the absence of ATP due to the strain on the motor head generated by the load. Nevertheless, we here focus on the ATP-driven stepping of kinesin motor and use logical operations to model how various [ATP] and loads perceived by the motor are transferred into mechanical steps. [ATP] is considered as a factor that affects the motor velocity at various loads,[21,22] and thus it is proposed as a mean for temporal control of synthetic nanodevices powered by kinesin motor.[12,34]

The four-state kinetic scheme of kinesin motor shows that the stepping completion times are correlated to the mean waiting time, t_i, in kinetic states[15]

$$t_i = 1/(u_i^F + w_i^F) \quad (5)$$

where the transition rates u_i^F and w_i^F are computed using eqs 1 and 2 and i = 0, 1, 2, 3. Using eq 5 we calculated the durations of the four kinetic states during the forward and backward stepping cycles under different [ATP] and loads (Figure 2A-D). Figure 2A shows that at low [ATP] and low loads the duration of kinetic state "0" is greater than that of other states which agrees with experimental findings since at limiting [ATP], kinesin is paused at kinetic state "0", waiting for ATP binding.[1,35] With increasing [ATP], the ATP binding rate raises which leads to a reduction in the duration of kinetic state "0" to eventually fall below the durations of states "2" and "3". It has been observed by Schnitzer et al.[21] that at limiting [ATP] the detachment probability of kinesin motor from MT in kinetic state "0" increases with the raise in the duration of this state, whereas at high [ATP] the detachment probability from kinetic state "0" diminishes. Accordingly, our results in Figure 2A-D suggest that at high [ATP] and all loads (similar to at all [ATP] and loads $F > 10$ pN) (*i*) kinetic states "2" and "3" are the most probable states for the detachment from MT due to their longer durations, as observed experimentally in refs 2 and 36−39, and (*ii*) kinetic state "2" is the most probable state for the detachment from MT at loads above 10 pN, in agreement with the experimental observations in refs 37 and 38. These results are also consistent with the weak affinity of kinesin to MT in kinetic states "2" and "3".[37,38] The detachment of kinesin motor from MT caused by regulatory factors (e.g., long pausing,[21] high backward loads,[24] obstacles on MT,[40] and the release of cargo[41]) autoinhibits its stepping motion.[42,43]

To compare the durations of weakly bound states "2" and "3", we analyze their respective kinetic transitions. With increasing load from high forward to backward: (*i*) forward rates u_2^F and u_3^F fall equally as they have the same parameters (see Table 1), whereas they are lower than the decreasing u_1^F (see Figure 1A), indicating that the rate limiting step of the ATPase cycle is P_i or ADP release in the presence of MTs[44] and (*ii*) backward w_2^F rises with a rate much smaller than w_3^F because $w_2^0 = 1.6\ s^{-1}$ is very small compared to $w_3^0 = 40\ s^{-1}$, meaning that the P_i binding rate is faster than the ATP synthesis rate, as reported by Hackney[31] (see eqs 1 and 2). Thus, according to eq 5, the slow rise of ATP synthesis rate, i.e. w_2^F, maximizes t_2 at a load and a time higher than those of t_3. This implies that under high backward loads $F > F_{stall}$ the ATP synthesis rate is inversely proportional to the duration of backward stepping cycles. Our analysis indicates that t_2 maximizes at 4657×10^{-6} s at load F = 10.946 pN suggesting 10.946 pN to be the load point where the detachment probability in kinetic state "2" is the highest, in accordance with the observations of Schnitzer and colleagues,[21] due to low rate of ATP synthesis. The load point 10.946 pN is

dx.doi.org/10.1021/ci500673z | J. Chem. Inf. Model. 2014, 54, 3439−3445

also consistent with the common detachment load $F_{detach} > 10$ pN observed by Carter and Cross.[24] Figure 2C further shows that t_2 decreases because of the fast rise of ATP synthesis rate at loads $F > 10.946$ pN deducing that with an increase in the rate of ATP synthesis at loads $F > F_{stall}$ (i) the detachment probability of kinesin motor from MT may decrease as t_2 diminishes and (ii) the velocity of backward stepping may increase.

2.2. Computational Model. To model the mechanical kinetics driving the forward and backward stepping cycles of kinesin motor at various [ATP] and loads using logical operations, we construct a FSM as an abstract computational model and use sequential logic to design a digital circuit. The state diagram of the circuit is constructed as a Mealy FSM,[17] $M_{kinesin}$, due to the correlation of the kinesin motor function to the perceived [ATP] and load from the cellular environment discussed in the previous section. To construct $M_{kinesin}$, we define and assign binary values to its inputs, outputs, and internal states according to the kinesin motor's perceived stimuli, stepping direction, and kinetic states, respectively. The $M_{kinesin} = (S, \sum, \prod, \delta, \varphi, s_0)$ consists of the following: (i) the set $S = \{s_0, s_1, s_2, s_3\}$ of states where s_0 to s_3 stand for the kinetic states "0" to "3", respectively, (ii) the input set $\sum = \{x_1, x_2\}$ where x_1 and x_2 stand for [ATP] and load, respectively, (iii) the output set $\prod = \{O_F, O_B\}$ where O_F and O_B stand for the forward and backward steppings, respectively, (iv) the transition function δ: $S \times \sum \rightarrow S$ which resembles kinetic transitions corresponding to ATP hydrolysis, (v) the output function φ: $S \times \sum \rightarrow \prod$ which represents the steppings, and (vi) the initial state s_0 which represents the initial state of the kinesin cycles, the kinetic state "0". The binary values 0 and 1 of input x_1 are assumed to correspond to 1 μM $\leq$ [ATP] $<$ 50 μM and 50 μM $\leq$ [ATP] $\leq$ 2 mM, respectively, representing relatively low and high [ATP] ranges, as usually applied in experimental and theoretical settings.[1,2,15,16,19,21,24,25,32,39] Input x_2 is supposed to reset to 0 at loads -10 pN $\leq F < F_{stall}$ and set to 1 at loads $F_{stall} < F \leq 10$ pN to denote the forward and backward stepping load ranges of kinesin motor, respectively. As at load $F = F_{stall}$ forward and backward steppings are equally likely, $F = F_{stall}$ can be considered to be in either $x_2 = 0$ or $x_2 = 1$. It is also supposed that kinesin motor only steps forward at loads $F < F_{stall}$ and backward at loads $F > F_{stall}$, as they are more likely to happen in these load ranges.[24,25] To represent the states of $M_{kinesin}$, we use two boolean variables to generate four states, y_1y_2 and Y_1Y_2, to denote the present and the next states of $M_{kinesin}$, respectively. We assign binary values to the internal states using Karnaugh map principles[45] in such a way that only one state variable (y_1 or y_2) changes when a state transition occurs (see Figure 2E). To assign binary values to outputs O_F and O_B, we follow the kinetic cycles of the forward and backward steppings. The individual forward and backward stepping cycles start in the kinetic state "0",[1,24] in states $y_1y_2 = 00$ or $Y_1Y_2 = 00$ of $M_{kinesin}$. The forward stepping cycle starts from kinetic state "0", and forward jump occurs when the kinetic state "3" changes to "0" at low or high [ATP] and loads $F < F_{stall}$. Accordingly, the output O_F of $M_{kinesin}$ is set to 1 when the present internal state $y_1y_2 = 10$ of $M_{kinesin}$ changes to the next state $Y_1Y_2 = 00$ with input $x_1x_2 = X0$, where the boolean variable X is equal to either 0 or 1. For backward stepping, the process initiates similarly from kinetic state "0" and completes with a backward jump when the kinetic state changes from "3" to "0" at low or high [ATP] but at loads $F_{stall} < F < F_{detach}$. Accordingly, the output O_B of $M_{kinesin}$ is set to 1 when the present internal state $y_1y_2 = 10$ changes to the next state $Y_1Y_2 = 00$ with input $x_1x_2 = X1$. We develop the state diagram of the circuit in Figure 2E and show that $M_{kinesin}$ perceives inputs x_1 and x_2 and produces outputs O_F and O_B, whereas its internal state changes in the sequence of $s_0 \rightarrow s_1 \rightarrow s_2 \rightarrow s_3 \rightarrow s_0$. Therefore, the state table corresponding to the outputs and next states of the sequential circuit in the presence of inputs and present states is shown in Table 2. Using Table 2, we compute the simplified boolean functions of state variables Y_1 and Y_2 as

$$Y_1 = y_2 \tag{6}$$

$$Y_2 = y_1' \tag{7}$$

Table 2. State Table Providing the Next States and Outputs[a]

present state		input		next state		output	output
y_1	y_2	x_1	x_2	Y_1	Y_2	O_F	O_B
0	0	0	0	0	1	0	0
0	0	0	1	0	1	0	0
0	0	1	0	0	1	0	0
0	0	1	1	0	1	0	0
0	1	0	0	1	1	0	0
0	1	0	1	1	1	0	0
0	1	1	0	1	1	0	0
0	1	1	1	1	1	0	0
1	0	0	0	0	0	1	0
1	0	0	1	0	0	0	1
1	0	1	0	0	0	1	0
1	0	1	1	0	0	0	1
1	1	0	0	1	0	0	0
1	1	0	1	1	0	0	0
1	1	1	0	1	0	0	0
1	1	1	1	1	0	0	0

[a]For example, the first row of the table shows that the present state $y_1y_2 = s_0 = 00$ of the circuit changes to the next state $Y_1Y_2 = s_1 = 01$ in response to the input $x_1x_2 = 00$. This behavior of the circuit corresponds to the kinetic state changing of kinesin motor from "0" to "1" at [ATP] $<$ 50 μM and loads $F < F_{stall}$.

Equations 6 and 7 show that the next state Y_1Y_2 of the circuit depends only on the present state y_1y_2, not on inputs x_1 and x_2. They indicate that the next kinetic state of kinesin motor is determined by the present kinetic state only, not on [ATP] and load F. This is due to that both forward and backward stepping cycles are associated with ATP hydrolysis process discussed in the previous section (see Figure 1). The simplified boolean functions of outputs O_F and O_B can also be obtained from Table 2 as

$$O_F = x_2'y_1y_2' \tag{8}$$

$$O_B = x_2y_1y_2' \tag{9}$$

The outputs O_F and O_B are set to 1 for forward and backward jumps of kinesin motor, respectively. Equations 8 and 9 show that the proposed circuit differentiates the stepping direction based on only input x_2. This result agrees with the experimental observations reported by Carter and Cross,[24] showing that the choice between forward and backward stepping depends only on load, not on [ATP]. To design the circuit, we synchronize the changes of the state variables Y_1 and Y_2 based on the present state variables y_1 and y_2 (see eqs 6 and 7). We use two

dx.doi.org/10.1021/ci500673z | J. Chem. Inf. Model. 2014, 54, 3439−3445

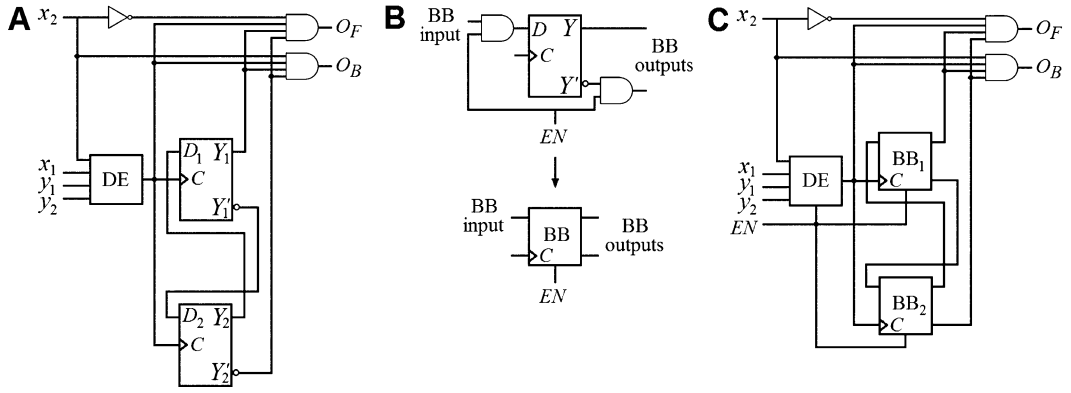

Figure 3. Circuit models. (A) Circuit for modeling the processing unit underlying stepping cycles of kinesin motor. The applied DE is programmed to provide delay t_i (see eq 5) in the control inputs of the D flip-flops. For clarity of the circuit, the connections between y_1y_2 and flip-flips' inputs are not shown. (B) Logic and block diagram of BB: input $EN = 0$ leads to reset inputs and complement outputs of the D flip-flops. With input $EN = 1$, inputs and outputs of BBs are equal to inputs and outputs of the D flip-flops, respectively. (C) Final circuit with BBs.

D flip-flops to synchronously store the 2-bit state variables. The D flip-flop is a basic digital circuit element that consists of one input data (D), one control input (C), and two outputs (Y and Y'). For the D flip-flop, the next state or output is equal to its input data when the control input C is triggered (see Figure 2F).[45] As the internal states of the circuit stand for the kinetic states of kinesin motor, the control inputs of the flip-flops should be triggered at intervals equal to the mean waiting times over the kinetic states of kinesin motor during forward and backward stepping cycles, t_i where $i = 0, 1, 2, 3$ (see eq 5). In this way, the active durations of circuit states will be equal to the delays t_i. In accordance with the theory of communicating mobile nanomachines in which the actions of each nanomachine are governed by its FSM's local clock,[46] we connect the control inputs of D flip-flops to a digitally programmable delay element (DE)[47] to provide the delay t_i in these control inputs. To program DE to provide the delay t_i, the present state y_1y_2 of the flip-flops and inputs x_1 and x_2 are arranged as inputs to the DE since t_i depends on the kinetic state of kinesin motor, [ATP], and load (see eq 5). Therefore, DE triggers the D flip-flops at intervals equal to t_i. DE is also connected to the outputs of the circuit to synchronize their setting to 1 and resetting to 0 with DE signals. This architecture provides a small active duration of outputs compared to the duration of stepping cycle because the moving time of kinesin in one step is about three orders smaller than the ATPase time.[48] The circuit designed using eqs 6−9 and D flip-flops are shown in Figure 3A.

The experimental observations have shown that in the presence of regulatory factors, the stepping motion of kinesin motor is deactivated as the motor's continuous kinetic state change is halted.[21,24,40−43] We model all such regulatory factors as an enable (EN) input signal which activates/deactivates the circuit function. The binary value of $EN = 0$ denotes the presence of regulatory factors, whereas $EN = 1$ defines the absence of regulatory factors and the attachment of kinesin motor to MT. To apply the input signal EN to the circuit in Figure 3A, it is connected to the voltage control of DE. It is also connected to the inputs and complement outputs of the D flip-flops through an AND gate, as the complement output of the second flip-flop is connected to the outputs O_F and O_B. We denote the resulting EN regulated flip-flops as binary block (BB) (see Figure 3B). The final circuit in Figure 3C indicates that input $EN = 0$ powers off DE and resets the inputs and complement outputs of BBs. Accordingly, it will reset the outputs O_F and O_B of the circuit. On the other hand, with input $EN = 1$, DE triggers active BBs in t_i intervals which leads to generate 1/0 signals in outputs O_F and O_B resembling the forward and backward steps of kinesin motor, respectively.

3. ANALYSIS AND DISCUSSION

The circuit in Figure 3C models the mechanical kinetics actuating the forward and backward stepping cycles of kinesin motor using logical operations. The model enables us to simulate the forward and backward steppings of the motor at various [ATP] and loads. We analyze the function of the circuit shown in Figure 3C with different input ranges and compare the results with the kinesin's mechanism. With input $EN = 1$, depending on the different ranges of inputs x_1 and x_2 as well as the circuit state, DE provides 16 various delay settings which define the active duration ranges of the circuit states (see Table 3). Different combinations of the four inputs of DE show that the highest maximum active duration belongs to state $y_1y_2 = 00$, i.e. t_0, with input $x_1x_2 = 0X$. With input $x_1x_2 = 00$, t_0 peaks at a maximum of 5209×10^{-4} s at $F = 0.75$ pN and [ATP] = 1. With increasing [ATP] and load, the active duration of state

Table 3. 16 Different Delay Ranges Provided by DE, Depending on Its Four Inputs

DE inputs				delay t (s)	
y_1	y_2	x_1	x_2	minimum	maximum
0	0	0	0	2388×10^{-7}	5209×10^{-4}
0	0	0	1	2958×10^{-8}	5687×10^{-5}
0	0	1	0	2439×10^{-8}	1207×10^{-5}
0	0	1	1	4083×10^{-9}	2177×10^{-6}
0	1	0	0	1145×10^{-6}	1662×10^{-6}
0	1	0	1	1058×10^{-6}	1605×10^{-6}
0	1	1	0	1145×10^{-6}	1662×10^{-6}
0	1	1	1	1058×10^{-6}	1605×10^{-6}
1	0	0	0	1962×10^{-6}	3032×10^{-6}
1	0	0	1	1331×10^{-6}	2589×10^{-6}
1	0	1	0	1962×10^{-6}	3032×10^{-6}
1	0	1	1	1331×10^{-6}	2589×10^{-6}
1	1	0	0	2298×10^{-6}	4445×10^{-6}
1	1	0	1	4119×10^{-6}	4636×10^{-6}
1	1	1	0	2298×10^{-6}	4445×10^{-6}
1	1	1	1	4119×10^{-6}	4636×10^{-6}

dx.doi.org/10.1021/ci500673z | J. Chem. Inf. Model. 2014, 54, 3439−3445

y_1y_2 = 00 decreases, whereas the active duration of state y_1y_2 = 11 becomes dominant (see Figure 2A, C) with a maximum of t_2 = 4636 × 10^{-6} s at F = 10 pN. These results are consistent with the obtained results of the mean waiting time over kinetic states and confirm that at limiting [ATP] kinesin mainly stays in kinetic state "0", whereas at high backward loads the duration of being in kinetic state "2" becomes dominant. These calculations suggest that the pausing of kinesin motor in kinetic state "0" at limiting [ATP] and low loads could be longer than that in kinetic state "2" at high loads. At limiting [ATP], the low rates of ATP and ADP binding cause the duration of kinetic state "0" to peak at F = 0.75 pN because of the direct proportionality of these rates to [ATP] (see eqs 1-5). The duration of kinetic state "2" is also maximized under high backward loads due to the low rate of ATP synthesis, as discussed in the previous section. These results accord with the greater rate of ATP synthesis under high backward loads in comparison with the rates of ATP and ADP binding when [ATP] and load are low (see eqs 1 and 2). These results are also consistent with our findings in ref 16 showing kinetic state "0" to be the most probable kinetic state for kinesin detachment from MT at low [ATP] and low loads, whereas at high [ATP] kinetic states "2" and "3" are the first and second most probable kinetic states for the detachment of kinesin from MT due to their longer durations. Therefore, on the basis of our results that both forward and backward stepping cycles are associated with ATP binding, it is found that the [ATP]-dependent duration of kinetic state "0" can change the motor velocity at fixed loads.

To verify that the circuit model simulates the single forward and backward stepping cycles of kinesin motor in response to the same biochemical stimuli, we explore the circuit behavior in response to inputs [ATP] = 100 μM and F = 1 pN in the absence of regulatory factors. As EN = 1, DE is active with the initial state y_1y_2 = 00 and recognizes the inputs x_1x_2 = 10. DE with input 0010 ($y_1y_2x_1x_2$) provides the delay t_0 = 6206 × 10^{-6} s over initial state y_1y_2 = 00 where $t_0 \in$ (2439 × 10^{-8}, 1207 × 10^{-5}). Then, DE triggers BBs which leads to changing the circuit state to y_1y_2 = 01 and the DE input to 0110 providing the delay t_1 = 1641 × 10^{-6} s over present state y_1y_2 = 01 where $t_1 \in$ (1145 × 10^{-6}, 1662 × 10^{-6}). After 1641 × 10^{-6} s, the circuit state and the DE input are changed to y_1y_2 = 11 and 1110 providing the delay t_2 = 3564 × 10^{-6} s in the range of 2298 × 10^{-6} s to 4445 × 10^{-6} s over the present state y_1y_2 = 11. The completion of the delay t_2 transitions the state of the circuit to y_1y_2 = 10 and, accordingly, the input of DE to 1010 providing t_3 = 3025 × 10^{-6} s in the range of 1962 × 10^{-6} s to 3032 × 10^{-6} s. Finally, in the next pulse, DE triggers BBs which leads to setting the output O_F to 1 and changing the circuit state to y_1y_2 = 00, and the cycle iterates again. A simulation of the circuit function is shown in Figure 4A which is consistent with the obtained results of the durations of kinetic states in Figure 2A-D. In the next cycle of the circuit function when the present state is y_1y_2 = 11, we increase the input F to 9 pN. It changes the DE input to 1111 and increases delay t_2 to 4576 × 10^{-6} s, in the range of (4119 × 10^{-6}, 4636 × 10^{-6}). The next pulse of DE transitions the internal state to y_1y_2 = 10 with t_3 = 1587 × 10^{-6} s in the range of (1331 × 10^{-6}, 2589 × 10^{-6}). After 1587 × 10^{-6} s, DE pulses and sets the output O_B to 1 and changes the state to y_1y_2 = 00 (see Figure 4B). The behavior of the circuit agrees with our theoretical results about the highest duration of kinetic state "2" under high backward loads as well as the experimental observations that under loads $F_{stall} < F < F_{detach}$ backward stepping are more likely to happen via ATP hydrolysis.[24,25] The theoretical results in Figure 2A, C and Table 3 also enable us to show the behavior of the circuit at various thresholds of inputs [ATP] and F ranges. Figure 2A indicates that the decreasing [ATP] to the concentrations less than 1 μM causes a significant increase in the delay t_0. Similarly, with increasing F to loads above 10 pN, delay t_2 rises (see Figure 2C). Accordingly, when input x_1 (or x_2) to the circuit crosses the minimum threshold of 1 μM (or maximum threshold of 10 pN), the generated delay t_0 (or t_2) overflows its range which would reset EN to 0 and thus deactivates the circuit's state transition in state y_1y_2 = 00 (or y_1y_2 = 11). This is consistent with the high detachment probability of kinesin motor from MT in kinetic states "0" at limiting [ATP][21] and is in agreement with our theoretical results about the high detachment probability of the motor from MT in kinetic states "2" due to high backward loads F > 10 pN. Through rebinding of kinesin motor to MT, the stepping cycle starts in kinetic state "0",[1,24] which is well modeled as the initial state y_1y_2 = 00 of the circuit when EN is set to 1.

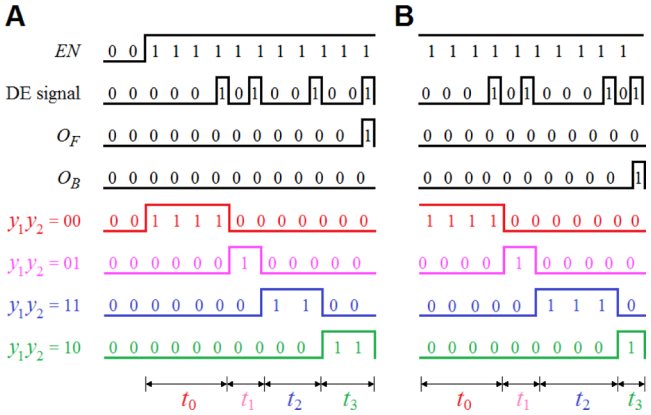

Figure 4. Simulation of two stepping cycles. In accordance with the state colors of $M_{kinesin}$ in Figure 2E, the durations t_0 to t_3 are shown in red, pink, blue, and green colors, respectively. (A) First cycle, inputs of the circuit are [ATP] = 100 μM and F = 1 pN. (B) In second cycle the input F is increased to 9 pN when the present state is y_1y_2 = 11.

In conclusion, our circuit model represents the mechanical kinetics actuating the forward and backward stepping cycles of kinesin motor as a four-state Mealy FSM driven by energy released from ATP hydrolysis. This model simulates the stepping behavior of the motor at various [ATP] and loads, in accordance with the in vivo data of kinesin. The proposed computational model suggests that in molecular communication the load that information molecules apply on the motor could be used to directionally transport bionanomachines carrying information molecules over a network of MTs, whereas [ATP] can be manipulated to control the duration and velocity of this transportation.

AUTHOR INFORMATION

Corresponding Authors

*E-mail: h.r.khataee@griffithuni.edu.au.

*E-mail: a.liew@griffith.edu.au.

Notes

The authors declare no competing financial interest.

ACKNOWLEDGMENTS

We thank Prof. Robert A. Cross for his careful reading and constructive feedback on the manuscript. This work is

supported by the International Postgraduate Research Scholarship (IPRS) and the Australian Postgraduate Award (APA) of Griffith University.

REFERENCES

(1) Clancy, B. E.; Behnke-Parks, W. M.; Andreasson, J. O. L.; Rosenfeld, S. S.; Block, S. M. A universal pathway for kinesin stepping. *Nat. Struct. Mol. Biol.* **2011**, *18*, 1020−1027.

(2) Yildiz, A.; Tomishige, M.; Gennerich, A.; Vale, R. D. Intramolecular Strain Coordinates Kinesin Stepping Behavior along Microtubules. *Cell* **2008**, *134*, 1030−1041.

(3) Yildiz, A.; Tomishige, M.; Vale, R. D.; Selvin, P. R. Kinesin Walks Hand-Over-Hand. *Science* **2004**, *303*, 676−678.

(4) Hess, H. Toward devices powered by biomolecular motors. *Science* **2006**, *312*, 860−861.

(5) Fischer, T.; Agarwal, A.; Hess, H. A smart dust biosensor powered by kinesin motors. *Nat. Nanotechnol.* **2009**, *4*, 162−166.

(6) Goodman, B. S.; Derr, N. D.; Reck-Peterson, S. L. Engineered, harnessed, and hijacked: Synthetic uses for cytoskeletal systems. *Trends Cell. Biol.* **2012**, *22*, 644−652.

(7) Sanchez, T.; Chen, D. T. N.; Decamp, S. J.; Heymann, M.; Dogic, Z. Spontaneous motion in hierarchically assembled active matter. *Nature* **2012**, *491*, 431−434.

(8) Nakano, T.; Moore, M. J.; Wei, F.; Vasilakos, A. V.; Shuai, J. Molecular communication and networking: Opportunities and challenges. *IEEE T. Nanobiosci.* **2012**, *11*, 135−148.

(9) Pierobon, M.; Akyildiz, I. F. A physical end-to-end model for molecular communication in nanonetworks. *IEEE J. Sel. Areas Commun.* **2010**, *28*, 602−611.

(10) Khataee, H. R.; Ibrahim, M. Y. Modelling of internal architecture of kinesin nanomotor as a machine language. *IET Nanobiotechnol.* **2012**, *6*, 87−92.

(11) Khataee, H. R.; Ibrahim, M. Y.; Liew, A. W. C. Flexible autonomous behaviors of kinesin and muscle myosin bio-nanorobots. *IEEE T. Ind. Electron.* **2013**, *60*, 5116−5123.

(12) Wang, J.; Manesh, K. M. Motion control at the nanoscale. *Small* **2010**, *6*, 338−345.

(13) De Silva, A. P.; Uchiyama, S. Molecular logic and computing. *Nat. Nanotechnol.* **2007**, *2*, 399−410.

(14) Wang, H. Several issues in modeling molecular motors. *J. Comput. Theor. Nanosci.* **2008**, *5*, 1−35.

(15) Khataee, H.; Liew, A. W. C. A mathematical model describing the mechanical kinetics of kinesin stepping. *Bioinformatics* **2014**, *30*, 353−359.

(16) Khataee, H.; Liew, A. W. C. A stochastic automaton model for simulating kinesin processivity. *Bioinformatics* **2014**, DOI: 10.1093/bioinformatics/btu664.

(17) Anderson, J. A. *Automata Theory with Modern Applications*; Cambridge University Press: New York, 2006; pp 99−114.

(18) Shiue, W.-T. Novel state minimization and state assignment in finite state machine design for low-power portable devices. *Integration* **2005**, *38*, 549−570.

(19) Fisher, M. E.; Kolomeisky, A. B. Simple mechanochemistry describes the dynamics of kinesin molecules. *Proc. Natl. Acad. Sci. U.S.A.* **2001**, *98*, 7748−7753.

(20) Kolomeisky, A. B.; Fisher, M. E. Molecular motors: A theorist's perspective. *Annu. Rev. Phys. Chem.* **2007**, *58*, 675−695.

(21) Schnitzer, M. J.; Visscher, K.; Block, S. M. Force production by single kinesin motors. *Nat. Cell Biol.* **2000**, *2*, 718−723.

(22) Visscher, K.; Schnltzer, M. J.; Block, S. M. Single kinesin molecules studied with a molecular force clamp. *Nature* **1999**, *400*, 184−189.

(23) Fisher, M. E.; Kim, Y. C. Kinesin crouches to sprint but resists pushing. *Proc. Natl. Acad. Sci. U.S.A.* **2005**, *102*, 16209−16214.

(24) Carter, N. J.; Cross, R. A. Mechanics of the kinesin step. *Nature* **2005**, *435*, 308−312.

(25) Nishiyama, M.; Higuchi, H.; Yanagida, T. Chemomechanical coupling of the forward and backward steps of single kinesin molecules. *Nat. Cell Biol.* **2002**, *4*, 790−797.

(26) Wang, H. A robust mathematical formulation for studying elastically coupled motor-cargo systems. *J. Comput. Theor. Nanosci.* **2006**, *3*, 922−932.

(27) Wang, H. A numerical algorithm for investigating the role of the motor-cargo linkage in molecular motor-driven transport. *J. Theor. Biol.* **2006**, *239*, 33−48.

(28) Wang, H.; Peskin, C. S.; Elston, T. C. A robust numerical algorithm for studying biomolecular transport processes. *J. Theor. Biol.* **2003**, *221*, 491−511.

(29) Hughes, J.; Hancock, W. O.; Fricks, J. A matrix computational approach to kinesin neck linker extension. *J. Theor. Biol.* **2011**, *269*, 181−194.

(30) Krishnan, A.; Epureanu, B. I. Renewal-Reward Process Formulation of Motor Protein Dynamics. *Bull. Math. Biol.* **2011**, *73*, 2452−2482.

(31) Hackney, D. D. The tethered motor domain of a kinesin-microtubule complex catalyzes reversible synthesis of bound ATP. *Proc. Natl. Acad. Sci. U.S.A.* **2005**, *102*, 18338−18343.

(32) Liepelt, S.; Lipowsky, R. Kinesin's network of chemomechanical motor cycles. *Phys. Rev. Lett.* **2007**, *98*, 2581021−2581024.

(33) Taniguchi, Y.; Nishiyama, M.; Ishii, Y.; Yanagida, T. Entropy rectifies the Brownian steps of kinesin. *Nat. Chem. Biol.* **2005**, *1*, 342−347.

(34) Dinu, C. Z.; Chrisey, D. B.; Diez, S.; Howard, J. Cellular motors for molecular manufacturing. *Anat. Rec.* **2007**, *290*, 1203−1212.

(35) Hackney, D. D. Evidence for alternating head catalysis by kinesin during microtubule- stimulated ATP hydrolysis. *Proc. Natl. Acad. Sci. U.S.A.* **1994**, *91*, 6865−6869.

(36) Hackney, D. D. Pathway of ADP-stimulated ADP release and dissociation of tethered kinesin from microtubules. Implications for the extent of processivity. *Biochemistry* **2002**, *41*, 4437−4446.

(37) Schliwa, M. *Molecular Motors*; Wiley-VCH: Weinheim, Germany, 2003; pp 253−257.

(38) Seitz, A.; Surrey, T. Processive movement of single kinesins on crowded microtubules visualized using quantum dots. *EMBO J.* **2006**, *25*, 267−277.

(39) Yajima, J.; Alonso, M. C.; Cross, R. A.; Toyoshima, Y. Y. Direct long-term observation of kinesin processivity at low load. *Curr. Biol.* **2002**, *12*, 301−306.

(40) Verhey, K. J.; Kaul, N.; Soppina, V. Kinesin assembly and movement in cells. *Annu. Rev. Biophys.* **2011**, *40*, 267−288.

(41) Hirokawa, N.; Noda, Y.; Tanaka, Y.; Niwa, S. Kinesin superfamily motor proteins and intracellular transport. *Nat. Rev. Mol. Cell Biol.* **2009**, *10*, 682−696.

(42) Friedman, D. S.; Vale, R. D. Single-molecule analysis of kinesin motility reveals regulation by the cargo-binding tail domain. *Nat. Cell Biol.* **1999**, *1*, 293−297.

(43) Kaan, H. Y. K.; Hackney, D. D.; Kozielski, F. The structure of the kinesin-1 motor-tail complex reveals the mechanism of auto-inhibition. *Science* **2011**, *333*, 883−885.

(44) Higuchi, H.; Muto, E.; Inoue, Y.; Yanagida, T. Kinetics of force generation by single kinesin molecules activated by laser photolysis of caged ATP. *Proc. Natl. Acad. Sci. U.S.A.* **1997**, *94*, 4395−4400.

(45) Mano, M. M. *Digital Design*, 3rd ed.; Prentice Hall: Upper Saddle River, NJ, 2001; pp 222−225.

(46) Wiedermann, J.; Petru, L. Communicating mobile nano-machines and their computational power. In *Proc. NanoNet*; Springer: 2009; Vol. 3 LNCS, pp 123−130.

(47) Maymandi-Nejad, M.; Sachdev, M. A Digitally Programmable Delay Element: Design and Analysis. *IEEE T. VLSI Syst.* **2003**, *11*, 871−878.

(48) Xie, P.; Dou, S. X.; Wang, P. Y. Mechanism for unidirectional movement of kinesin. *Chin. Phys.* **2005**, *14*, 734−743.